Article

Not peer-reviewed version

Alterations of Cerebral Extracellular Vesicle microRNA Profiling Potentially Disrupts Brain Homeostasis Following Myocardial Infarction

MD Monowarul Islam [†] , Shouyi Liang [†] , Lijun Sun , Guoku Hu , Neha Dhyani , Lie Gao , Tara L. Rudebush , Xue Xu , Jinpeng Liu , Irving H. Zucker , Changhai Tian [*]

Posted Date: 8 May 2026

doi: 10.20944/preprints202605.0455.v1

Keywords: heart failure; cognitive impairment; cerebral extracellular vesicle; oxidative stress; neuroinflammation

 doi:10.20944/preprints202605.0455.v1

Article

Alterations of Cerebral Extracellular Vesicle microRNA Profiling Potentially Disrupts Brain Homeostasis Following Myocardial Infarction

MD Monowarul Islam [1,†], Shouyi Liang [2,†], Lijun Sun [1], Guoku Hu [3], Neha Dhyani [5], Lie Gao [4], Tara L. Rudebush [5], Xue Xu [1], Jinpeng Liu [2], Irving H. Zucker [5] and Changhai Tian [1,*]

[1] Department of Toxicology and Cancer Biology
[2] Department of Cancer Biostatistics, University of Kentucky, Lexington, KY 40536
[3] Department of Pharmacology and Experimental Neuroscience
[4] Department of Anesthesiology
[5] Department of Cellular and Integrative Physiology, University of Nebraska Medical Center, Omaha, NE 68198
* Correspondence: tch815@uky.edu; Tel.: 859-562-0290; Fax: (859) 323-1059
† These authors contributed equally to this work.

Abstract

Cognitive impairment (CI) is prevalent among heart failure (HF) patients. Although the brain injury in HF is multifactorial, oxidative stress and neuroinflammation are common pathological features of neurological disorders and are increasingly recognized as key underlying mechanisms of CI. The role of extracellular vesicles (EVs) as effective communicators of biological signaling in myocardial function has been extensively investigated. EVs are well-known to transport a variety of microRNAs (miRNAs), however, it is unclear if myocardial injury alters the miRNA profiling of brain EVs which may contribute to CI by disrupting brain homeostasis. Using a rodent myocardial infarction (MI) model, we isolated brain EVs, and characterized their miRNA profiling by small RNA sequencing. Our results demonstrate that miRNA profiling in brain EVs varies with the progression of HF. Only three miRNAs were significantly changed at 3wks post-MI, thirty-two miRNAs demonstrate significant changes at 6wks post-MI, and sixty-five miRNAs show significant alterations at 12wks post-MI. Bioinformatic analysis suggests that some miRNAs against oxidative stress and inflammation were downregulated in brain EVs following 6wks post-MI, whereas several miRNAs responsible for oxidative stress and neuroinflammation were significantly increased, which may be cardiac in origin following MI. Collectively, cardiac EVs may contribute to the miRNA alterations in brain EVs, potentially contributing to CI by disrupting brain homeostasis.

Keywords: heart failure; cognitive impairment; cerebral extracellular vesicle; oxidative stress; neuroinflammation

1. Introduction

Cardiovascular disease including heart failure (HF) remains the leading cause of mortality and impacts health and economic burden in the United States and worldwide [1]. Furthermore, clinical and experimental evidence suggest that 20%-80% of patients with myocardial ischemia are affected by cognitive impairment (CI) such as memory and global cognitive deficits [2,3]. However, the underlying mechanisms by which ischemic myocardial injury contributes to the progression of CI remain elusive.

CI has been clinically reported in patients with different cardiac diseases including hypertension, atrial fibrillation and coronary artery diseases [2]. It is well-documented that cerebral blood flow (CBF) declines with increasing age [4,5] and has been implicated in the occurrence of CI

 doi:10.20944/preprints202605.0455.v1

among elderly patients with HF. Gradual disruptions in cerebral hemodynamics appear to play a critical role in the pathogenesis of CI [6-8]. Although decreased CBF is a major contributor, CI has also been observed in the progression of HF, regardless of CBF impairment [9-11]. This suggests that other mechanisms may contribute to CI in response to myocardial injury. Extracellular vesicles (EVs) have been increasingly recognized as mediators for intra- and inter-organ communication in human diseases [12-14]. Some bioactive materials, including lipids, proteins and nucleotides such as non-coding RNAs are abundant in EVs and play important roles in the pathogenesis of human diseases, including HF [15-17]. Recent studies from our laboratory and others have demonstrated that cardiac EV-mediated heart-brain axis crosstalk contributes to brain structural damage [18], oxidative stress [19] and neuroinflammation [20,21]. Cardiac EV-enriched miRNAs play critical roles in these pathophysiological processes in the brain following myocardial infarction (MI) [18-20]. Given that cardiac-derived miRNAs are potentially involved in disrupting brain homeostasis in HF, it remains unclear whether the miRNA expression profiling of cerebral EVs varies during the progression of HF, and if cerebral EV-enriched miRNAs are of cardiac origin and responsible for cerebral oxidative stress and neuroinflammation causing CI.

Here, we hypothesize that cardiac EVs are abundant with miRNAs which are dysregulated following myocardial infarction (MI), and circulate to the brain where miRNAs regulate brain oxidative stress and neuroinflammation contributing to CI. To address this hypothesis, we investigated changes in miRNA profiles in brain tissue-isolated EVs following the progression of HF using a rat model. We analyzed the relationship between dysregulated miRNAs of brain EVs at different time points post-MI and cerebral pathological changes including oxidative stress, neuroinflammation and neuronal damage.

2. Materials and Methods

2.1. Rat model of Heart Failure

Male Sprague-Dawley rats (180–200 g) were used to generate chronic HF. model by the ligation of left anterior descending coronary artery As previously described [22], the left anterior descending coronary artery was ligated following a left thoracotomy under isoflurane anesthesia (2%), and sham animals underwent a similar surgical procedure without coronary artery ligation. Long-acting Buprenorphine ER (1.2 mg/kg, sc) was used as analgesia during recovery from surgery. All experimental rats were subjected to echocardiography to determine cardiac function using a Vevo 3100 Imaging System with a 40 MHz probe (Visual Sonics, Inc.) at 3 weeks, 6 weeks, and 12 weeks post-myocardial infarction (MI), respectively [19]. MI animals with ejection fraction (EF%) more than 40 were excluded from further study. At the end of the study for each animal, hemodynamic measurements were made using a Millar pressure catheter inserted into the left ventricle through the right carotid artery under 2% isoflurane anesthesia. All animal experimental protocols were approved by the Institutional Animal Use and Care Committee (IACUC) at the University of Nebraska Medical Center and at the University of Kentucky and were carried out in accordance with the NIH Guidelines for the Care and Use of Laboratory Animals and with ARRIVE guidelines.

2.2. EV Isolation

Brain tissue EV isolation. Brain EVs were isolated from the Sham and HF rats as described previously [23,24] with modifications. Briefly, hemi-brain tissues were minced and treated with 20 units/ml papain in Hibernate A solution (ThermoFisher Scientific) at 37 °C shaker for 15 min, and then gently homogenized in cold Hibernate A solution. The brain homogenates were filtered with a 40 μm cell strainer and then followed by sequential centrifugations (300 x g for 30 min at 4 ºC; 2000 × g for 30 min at 4 ºC, and 10,000 × g for 30 min at 4 ºC) to discard cells, membranes and debris. The supernatants were filtered through a 0.22 μm syringe filter, and then followed by ultracentrifugation at 100,000 × g for 90 min at 4 ºC to pellet EVs. EVs were stored at -80 ºC.

 doi:10.20944/preprints202605.0455.v1

Cardiac EV isolation. Myocardial EV isolation was performed as previously described [25,26] with some modifications. Briefly, the heart was transcardially perfused with Phosphate-buffered saline (PBS), and the non-infarcted area of Left ventricle was minced (30 seconds, 4°C) using fine sterile scissors (2 cm strait blade) in pre-cold PBS (100 μL per 100 mg tissue), followed by digestion in 0.1% type II collagenase (Sigma-Aldrich, USA) at 37°C for 30 min. The digested tissue was centrifuged twice at 400 × g for 15 min to remove the tissues and cells, and the supernatant was subjected to ultracentrifugation at 100,000 x g for 90 min at 4°C to pellet all EVs after filtration with 0.45 μm sterile filters (Optima L-100XP Ultracentrifuge, Beckman Coulter). The EVs were obtained and resuspended in 100 μL PBS.

Plasma EV isolation. Total EVs of serum were isolated using a total EV isolation reagent (Cat. 4478360, Invitrogen) following the manufacturer's manual.

2.3. RNA extraction of brain EVs and miRNA sequencing

Total RNA including miRNA was extracted from brain tissue-derived EVs of Sham and HF rats using miRNeasy (QIAGEN). All extracted RNA was used in the library preparation following Illumina's TruSeq-small-RNA-sample preparation protocols (Illumina, San Diego, CA, USA). Quality control analysis and quantification of the DNA library were performed using Agilent Technologies 2100 Bioanalyzer High Sensitivity DNA Chip. Single-end sequencing 50 bp was performed on Illumina's Hisses 2500 sequencing system following the manufacturer's recommended protocols.

miRNA Sequencing and Bioinformatics analysis: Raw reads were processed and quantified using the in-house ACGT101-miR pipeline (LC Sciences, Houston, TX, USA). Briefly, adapter dimers, low-quality reads, low-complexity sequences, and reads corresponding to common RNA families (rRNA, tRNA, snRNA, snoRNA) and repetitive elements were removed. Clean reads with lengths between 18–26 nucleotides were aligned to species-specific precursor and mature miRNA sequences in miRBase v22.0 [27], allowing for one internal mismatch and length variation at the 3' or 5' ends. Only miRNAs matching the reference species were retained for quantification and downstream analysis.

Analysis of Differential expressed miRNAs: Differential expression analysis of miRNAs was performed using the DESeq2 package in R [28]. Differentially expressed (DE) miRNAs were defined as those with an absolute log fold change $|\log2(FC)| > \log2(1.5)$ and a false discovery rate FDR < 0.05.

The Prediction of Target Genes of miRNAs: Target genes of the DE miRNAs were identified using the multiMiR R package [29], integrating miRTarBase [30], TargetScan [31], and miRDB [32]. Functional enrichment analysis was performed on the identified target genes for each DE miRNA using the clusterProfiler package [33], focusing on Gene Ontology (GO) biological process terms. GO terms with a false discovery rate (FDR) less than 0.05 were considered statistically significant.

2.4. Quantitative Reverse Transcription Polymerase Chain Reaction (qRT-PCR)

Total RNAs were extracted and purified with TRIzol Reagent and miRNeasy Mini Kit (QIAGEN) from myocardial and plasma derived EVs per the manufacturer's recommendations. For miRNA analysis, a synthetic cel-miR-39 (IDT, Iowa) was pre-loaded to each denatured sample as a spike-in control to normalize the variation between samples during EV RNA extraction, and the reverse transcription of total RNA was performed using a TaqMan miRNA reverse transcription kit (Applied Biosystems, CA), per the manufacturer's protocol. The relative expressions of miRNAs and cel-miR-39 were quantified by using TaqMan mature miRNA assays (Applied Biosystems, CA) according to the manufacturer's protocol and using the $2^{(-\Delta\Delta Ct)}$ method.

2.5. Statistical Analysis

All data are presented as mean ± standard error of the mean (±SEM). The normality of all data sets was tested using the Kolmogorov-Smirnov and Shapiro-Wilk tests when sample size was more than six ($n \geq 6$). A non-parametric test was carried out to compare two groups if the sample size was less than six ($n < 6$). Unpaired t-tests were used to compare data between two groups with Welch's

 doi:10.20944/preprints202605.0455.v1

correction. One-way analysis of variance (ANOVA) was used for multiple comparisons using GraphPad Prism 9.2 software. P values less than 0.05 were considered statistically significant.

3. Results

3.1. Myocardial Infarction Alters the miRNA Profiling of Cerebral EVs

Hemodynamic and echocardiographic evaluation of the post MI HF model used here showed significant decreases in ejection fraction (EF%, **Figure 1A**) and fraction shortening (FS%, **Figure 1B**) in a time-dependent manner, beginning at 3 wks post-MI and peaking at 6 wks post-MI and stabilizing at 12 wks post-MI. Other parameters of chronic HF including Left Ventricular End-Diastolic Pressure (LVEDP, **Figure 1C**), Left ventricular end-diastolic volume (LVEDV, **Figure 1D**) and Left ventricular end-systolic volume (LVESV, **Figure 1E**) which were all significantly increased at 3 wks post-MI, and peaked at 6 wks post-MI and stabilized at 12 wks post-MI. Consistently, left-ventricular maximum rate of pressure increase (dp/dtmax) and decrease (dp/dtmin) exhibited significant differences in a time-dependent manner and then stablized at 12 wks post-MI (**Figure 1F**). As critical hemodynamic markers in heart failure, these experimental rats exhibit the highly negative correlation between LVEDP and EF (%) (**Figure 1G**). Based on these echocardiographic and hemodynamic analyses, we selected four individual brains with typical HF phenotypes as biological repeats (Supplemental **table 1**) from each group (Sham, 3wks, 6wks and 12wks post-MI) for brain EV isolation following the outline illustrated in **Figure 2A**. Transmission Electron Microscopy (TEM) shows the typical cup-shaped morphologies of brain-isolated EVs (**Figure 2B**), and quality control of total RNAs extracted from brain EVs of each group suggest that all RNAs consist of fragments ranging from 20 to 200 nucleotides in addition to the 18S and 28S nucleotide fragments (**Figure 2C**), which are suitable for miRNA sequencing.

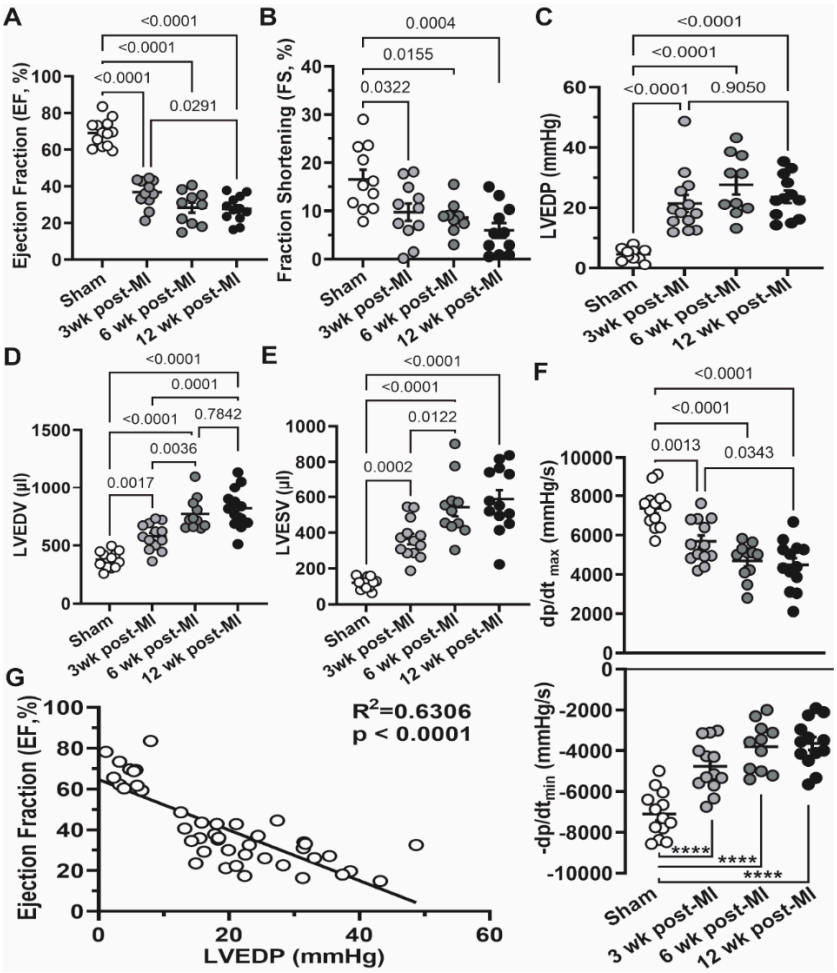

 doi:10.20944/preprints202605.0455.v1

Figure 1. Echocardiographic and hemodynamic analyses demonstrate the heart failure phenotype. Echocardiographic and hemodynamic analyses were performed using Sham and MI rats at 3wks, 6wks and 12wks post-MI, respectively. Ejection Fraction (A), Fraction shortening (B); Left ventricular end diastolic pressure (LVEDP) (C), left ventricular end diastolic volume (LVEDV) (D); left ventricular end systolic volume (LVEDV) (E) and $dp/dt_{max/min}$ (F) were measured. The correlation between EF (%) and LVEDP (mmHg) was also analyzed (G). Tests were carried out for normality with the Kolmogorov-Smirnov tests, and p values were derived from Brown-Forsythe and Welch ANOVA tests (parametric test) (n=10, ± SEM).

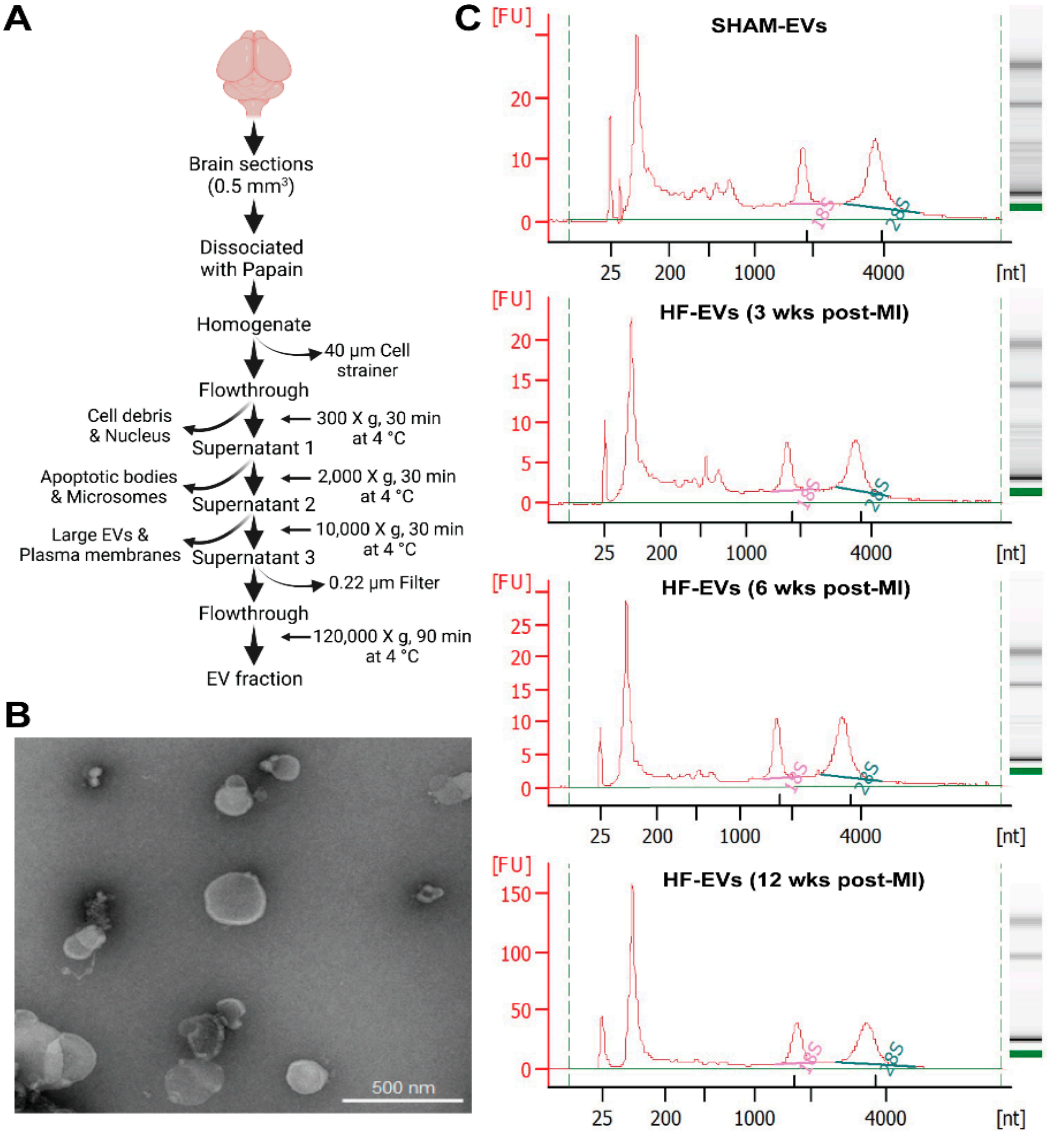

Figure 2. Pipelines for Brain isolated EVs and total RNA quality control of EVs. EVs were isolated from hemi-brain of Sham and MI rats, respectively at 3wks, 6wks and 12wks post-MI following the illustrated procedures (A); Morphology of isolated brain EVs by TEM (B) and quality control of total RNAs (C). (n=4/group).

We extracted miRNA data from Sham-EVs and HF-EVs at different time post MI points for analysis. Differential expression analysis of miRNAs between Sham-EVs and HF-EVs was determined using a threshold of $|\log2 \text{ fold change}| > 0.585$ and FDR < 0.05. Two miRNAs including miR-7b and miR-7a-5p were significantly decreased whereas only one miRNA, miR-3550, was in higher abundance in cerebral EVs at 3wks post-MI compared to the Sham group (**Figure 3A**). However, the number of dysregulated miRNAs enriched in the EVs isolated from the brain tissue increased relative to the progression of HF. 11 out of 32 dysregulated miRNAs were significantly increased in brain tissue EVs at 6wks post-MI. These included miR-125b, miR-543 and miR-342-3p (**Figure 3B**). Although all cardiac dysfunctional parameters were stabilized at 6wks post-MI, 29 out

 doi:10.20944/preprints202605.0455.v1

of 65 dysregulated miRNAs were still highly enriched in brain tissue EVs at 12wks post-MI compared to Sham group (**Figure 3C**).

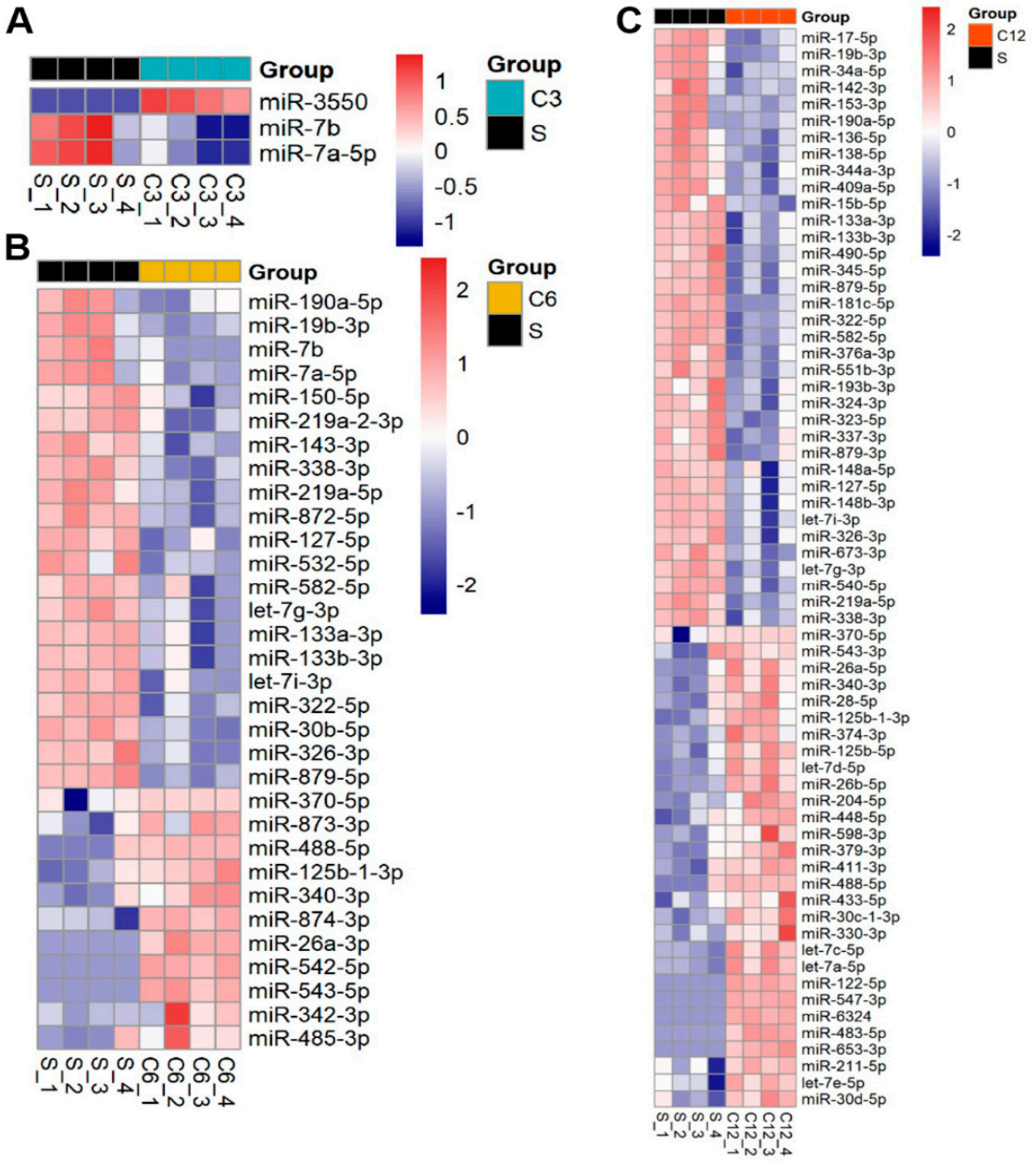

Figure 3. Differentially expressed miRNAs at 3, 6, and 12 weeks post-MI compared with Sham-operated controls. Heatmaps show the top differentially expressed miRNAs ranked by fold change from four biological samples at each time point: (A) Sham vs 3wks post-MI; (B) Sham vs 6wks post-MI; (C) Sham vs 12wks post-MI (n=4/each group). Up-regulated and down-regulated miRNAs are represented by red and blue colors, respectively. Thresholds of an absolute log fold change $|\log2(FC)| > \log2(1.5)$ and a false discovery rate FDR < 0.05 were universally applied.

3.2. Brain Tissue EV-Enriched miRNAs Are Involved in Central Pathological Alterations

To further confirm if these dysregulated miRNAs in brain tissue-isolated EVs contribute to the progression of cognitive impairment following the establishment of chronic HF, we performed Gene Ontology (GO) enrichment analysis for DE miRNAs at 6wks and 12wks post-MI, compared with Sham controls. The bioinformatic analyses suggest that 4 out of 17 upregulated miRNAs in brain EVs at 6wks post-MI demonstrate positive correlation with oxidative stress and neuroinflammation,

 doi:10.20944/preprints202605.0455.v1

including miR-488-5p, miR-26a-3p, miR-370-5p and miR-342-3p, in contrast, 13 out of 17 downregulated miRNAs were negatively related with oxidative stress, neuroinflammation and neuronal dysfunctions. These included miR-338-3p, miR-582-5p and miR-30b-5p (**Figure 4A**). However, the number of miRNAs contributing to neuronal dysfunction, learning or memory impairment, oxidative stress and neuroinflammation increased in brain EVs at 12wks post-MI. 20 out of 43 miRNAs enriched in brain tissue-isolated EVs, including miR-125b, miR-330-3p and miR-543-3p, contribute to these pathological alterations in chronic HF. The number of protective miRNAs potentially involved in these pathological alterations also increased but t were significantly downregulated (**Figure 4B**). These included miR-138-5p, miR-34a-5p and miR-338-3p.

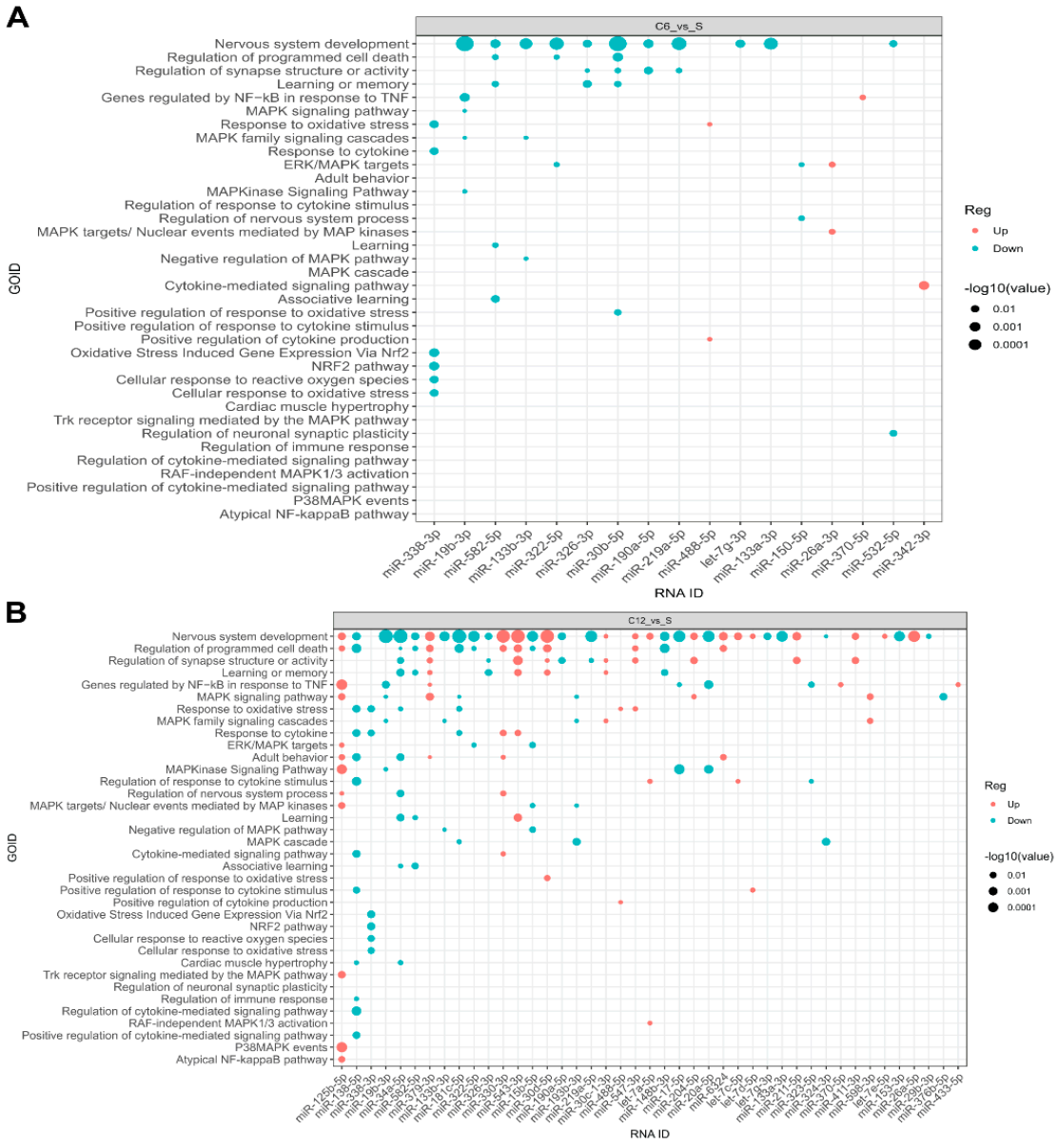

Figure 4. Gene Ontology (GO) enrichment analysis of the predicted target genes of differentially expressed miRNAs at 6 and 12 weeks post-MI compared with sham-operated controls. Bubble plots illustrate the enriched GO biological process terms of miRNA target genes, with the circle size corresponding to the enrichment significance -log$_{10}$FDR and the circle color indicating the direction of miRNA regulation (red for upregulated and blue for downregulated). Panel A shows the enrichment results for 6wks post-MI *vs* Sham, and Panel B for 12wks post-MI *vs* Sham. Enriched GO terms with FDR < 0.05 were considered statistically significant.

 doi:10.20944/preprints202605.0455.v1

3.3. Brain Tissue EV-Enriched miRNAs Are Potentially of Cardiac Origin

To validate the potential cardiac origin of these upregulated miRNAs in brain tissue-isolated EVs, we isolated the cardiac EVs from non-infarcted myocardium of left ventricles at 3wks, 6wks and 12wks post-MI, respectively, and the corresponding areas in the Sham-operated group as illustrated in **Figure 5A**. We then selectively detected several upregulated miRNAs in cerebral EVs and in cardiac EVs by qRT-PCR, including miR-125b, miR-543, miR-342-3p, miR-122, miR-30d and miR-330. The results demonstrated that miR-543, miR-342-3p and miR-125b levels were significantly upregulated in cardiac EVs at 6wks post-MI (**Figure 5D, 5E and 5F**), which is consistent with that observed in cerebral EVs at 6wks post-MI. Consistently, miR-122 and miR-30d levels significantly increased in cardiac EVs at 12wks post-MI (**Figure 5B and 5C**). However, although miR-330 was significantly increased in cerebral EVs at 12wks post-MI, this was not observed in cardiac EVs at 12wks post-MI but were significantly increased at 3wks and 6wks post-MI in a time-dependent manner (**Figure 5G**).

To further confirm the possibility that cerebral EV-enriched miRNAs may circulate from the heart following MI-induced HF, we collected circulating EVs from plasma samples as illustrated (**Figure 6A**). Interestingly, we observed that miR-125b was gradually upregulated in circulating EVs at 6wks and 12wks post-MI. This is consistent with the miR-125b level observed in both cardiac EVs and cerebral EVs following MI (**Figure 6B**). Moreover, miR-122 and miR-30d were also highly abundant in circulating EVs at 12wks post-MI, which were consistently observed in both cardiac EVs and cerebral EVs (**Figure 6C and 6F**). Furthermore, miR-342-3p level was highly enriched in circulating EV at 6wks post-MI as observed in cardiac and cerebral EVs (**Figure 6D**). Although miR-330 was not altered in circulating EVs as observed in cerebral EVs at 12wks post-MI, it was significantly increased at 6wks post-MI (**Figure 6E**).

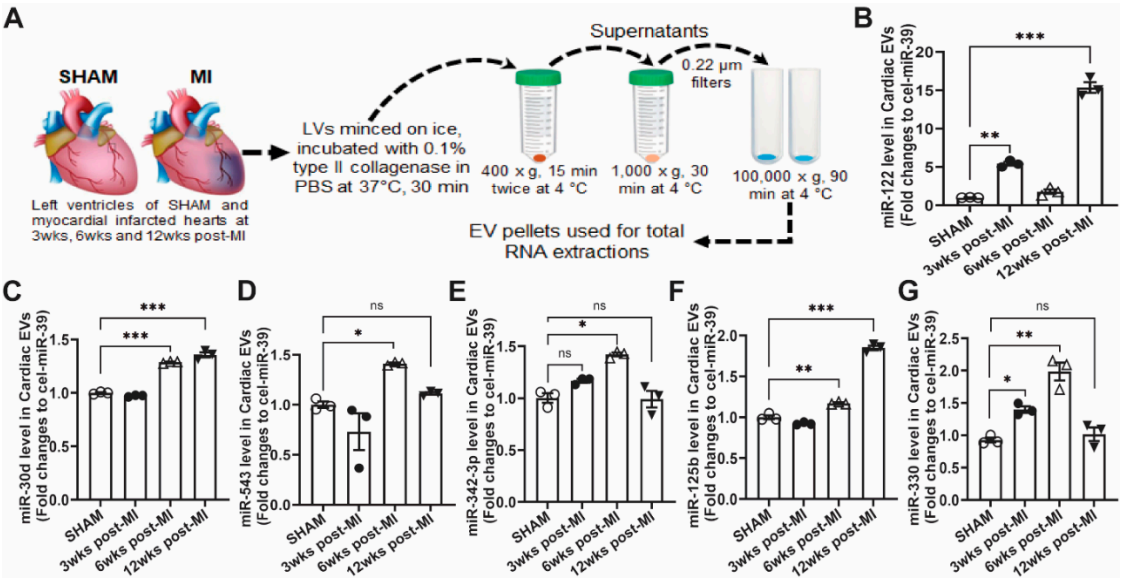

Figure 5. Cardiac miRNA profiling alterations following myocardial infarction. Cardiac EVs were isolated from the left ventricles of Sham, 3wks, 6wks and 12 wks post-MI rats, and then subjected to total RNA extraction, respectively, as illustrated procedures (A); qRT-PCR analysis was performed with miRNA primers specific to miRNA-122 (B), miRNA-30d (C), miRNA-543 (D), miRNA-342-3p (E), miR-125b (F) and miRNA-330 (G). Cel-mir-39 was loaded as a spike-in control (n=3, ± SEM). *denotes p <0.05; **denotes p<0.001 and ***denotes p<0.0001.

 doi:10.20944/preprints202605.0455.v1

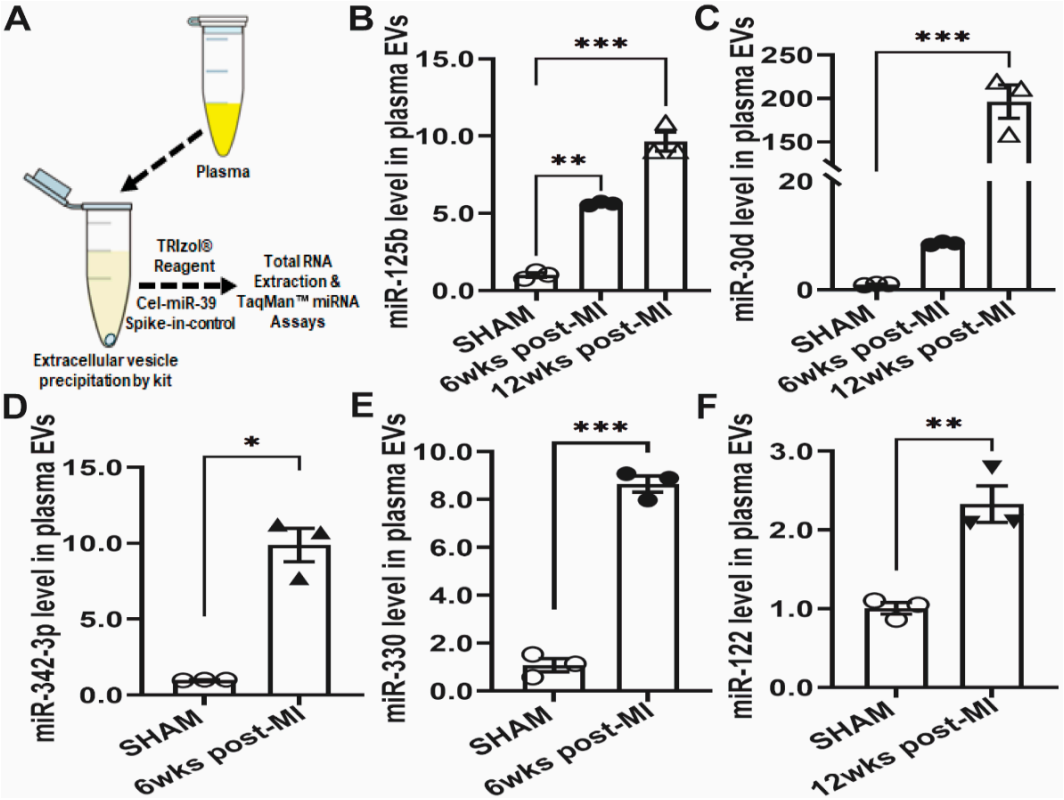

Figure 6. miRNA levels in plasma following myocardial infarction. Circulating EVs were isolated from plasma collected from sham and MI animals at 6wks and 12wks post-MI rats, respectively as illustrated procedures (A). qRT-PCR analyses show the miRNA-125b level (B) and miR-30d level (C) in plasma EVs of 6wks and 12wks post-MI, miRNA-342-3p level (D) and miRNA-330 level (E) in plasma EVs of 6wks post-MI, and miRNA-122 level (F) in plasma EVs of 12wks post-MI, cel-mir-39 was used as a spike-in control (n=3, ±SEM). *denotes $p < 0.05$; **denotes $p < 0.001$ and ***denotes $p < 0.0001$.

4. Discussion

Cognitive impairment (CI) and cardiogenic dementia are associated with a range of cardiovascular diseases including heart failure [2,11]. Studies show that 20-80% of patients with heart failure experience some form of cognitive decline, underscoring the high prevalence of CI [34-36]. However, the underlying mechanisms causing cognitive decline in heart failure patients remain to be elucidated. In the present study, we demonstrate that miRNA profiling in cerebral extracellular vesicles significantly alters following the progression of heart failure, and the number of dysregulated miRNAs increased in a time-dependent manner. Moreover, bioinformatics analysis revealed that those dysregulated miRNAs of cerebral EVs at late stages of heart failure are highly associated with neuronal dysfunction, oxidative stress and neuroinflammation. Furthermore, the results of qRT-PCR show that those upregulated miRNAs in cerebral EVs isolated at different time points in the progression of HF are abundant in cardiac and circulating EVs, respectively, suggesting that cardiac EVs encapsulated with miRNAs may act as mediators that connect heart and brain in the progression of HF and eventually contributing to cardiogenic dementia in heart diseases. Our studies provide novel insights into the pathogenic mechanism underlying the inter-organ crosstalk between heart and brain and suggest new therapeutic strategies for mitigating brain lesions to protect cognitive decline in management and treatment of HF.

The pathophysiological mechanism of cardiogenic dementia is complex and characterized by reciprocal interactions between the heart and the brain, leading to brain structural changes, oxidative stress and neuroinflammation [18,20,21,37]. Emerging evidence suggests that subclinical changes in the cardiovascular system contribute to brain injury and cognitive vulnerability even in the absence

 doi:10.20944/preprints202605.0455.v1

of overt disease through several interconnected signaling pathways. These include neural [38], hormonal signaling [39,40], the renin-angiotensin system [41,42], systemic inflammation [43,44] and oxidative stress [45,46]. Our previous studies provide evidence that EVs derived from the injured heart also serve as novel carriers for delivering bioactive materials, especially miRNAs, and mediate heart-brain communication [19,20]. These findings underscore cardiac EVs as a pathogenic factor contributing to the development of CI following MI and the generation of chronic HF. Although cardiac EV-enriched miRNAs have been implicated in the disruption of brain homeostasis following MI [18-20], the dynamic alterations of cerebral EV-enriched miRNA profiling in the progression of HF remain to be elusive. Here, we used a rat MI model that exhibits typical pathological phenotypes of HF, reaching stable at 12wks post-MI (Fig.1). Interestingly, we observed that three miRNAs were significantly dysregulated, but only one of the three was upregulated in cerebral EVs (Fig.3). It has been well-documented that both miR-7a-5p and miR-7b demonstrate neuroprotective roles in neurological disorders, such as Parkinson's disease and Alzheimer's disease [47-49]. However, they were significantly reduced in cerebral EVs at 3wks post-MI, suggesting that cardiac ischemia initially disrupts brain function at an early stage of HF. Although miR-3550 upregulation was observed in cerebral EVs, this miRNA is only expressed in rats and is positively associated with the development of Diabetic nephropathy [50].

With the progression of HF, most pathological phenotypes of HF reached a peak at 6wks post-MI (Fig.1). On the other hand, the dysregulated miRNA profile of cerebral EVs was altered early following MI (Fig.3). It has been well-known that miR-133a and miR-133b, also called muscle-specific miRNAs are specifically expressed in cardiac and skeletal muscle and play protective roles in regulating oxidative stress and inflammation within the CNS following MI or in neurological disorders [51-53]. In addition to miR-133a and miR-133b, we also observed that the abundance of other miRNAs, such as miR-219-5p, miR-338-3p and miR-150-5p are lower in cerebral EVs at 6wks and 12wks post-MI compared to Sham groups (Fig.3). Importantly, these miRNAs have been reported to have protective effects against oxidative stress and neuroinflammation [54-56]. In addition, some upregulated miRNAs were also enriched in cerebral EVs following MI and have been demonstrated to have detrimental effects through targeting oxidative stress and neuroinflammation (Fig. 4). For example, miR-125b-1-3p, which often functions alongside miR-125b has been reported to act as a critical regulator of inflammation and oxidative stress [57,58]. As a critical regulator of oxidative stress and inflammation, miR-122 upregulation has been found to promote pathological progression in neurological disease [59], heart disease [60] and liver disease [61,62] also through regulating oxidative stress and inflammation. These findings further confirm that cerebral EV-enriched dysregulated miRNAs contribute to the pathogenesis of CI following MI over time.

EVs have been emerging as mediators of inter-organ communication in the pathogenesis of human diseases [13,63,64]. Our recent studies have demonstrated cardiac EV-mediated heart-brain crosstalk following MI [19,20]. These studies and those from others also show that cardiac EV-enriched miRNAs not only elicit sympathetic excitation in brain stem nuclei through disrupting redox homeostasis but also cause structural damage by targeting hippocampal microtubules [18,19]. Here we profile miRNA alterations in cerebral EVs following the progression of HF, and further validate the potential cardiac origin of these cerebral EV-enriched miRNAs (Fig.5 and Fig. 6). These data support the hypothesis that cardiac EVs may contribute to the pathogenesis of cardiogenic dementia following MI through disrupting brain redox homeostasis and neuroinflammation by delivering cardiac miRNAs. This study not only provides new insights into the mechanism by which the damaged heart regulates brain function, but also provides promising therapeutic targets for HF treatment and management.

Limitations: There are several limitations that should be acknowledged. First, this study highlights only the importance of miRNAs enriched in cardiac-derived EVs in the pathogenesis of cardiogenic dementia, while overlooking the potential roles of other bioactive components in both early and later stages of HF. Second, although cardiomyocytes account for 40% of the cardiac cellular population, the cellular origin of cardiac EV-enriched miRNAs remain to be investigated. Third, the

 doi:10.20944/preprints202605.0455.v1

brain targets and functions of these upregulated miRNAs in cerebral EVs remain to be further confirmed. Fourth, the study did not evaluate cognitive ability by behavioral testing post-MI, and didn't test potential treatment with antagomirs of these dysregulated miRNAs in HF.

Author Contributions: Conceptualization, C.T.; Methodology, M. I., S.L., L.S., G. H., N.D., L.G., T. L. R., X.X. and J. L.; Software, S. L. and J.L.; Validation, C.T., L.S. X.X. and M.I.; Writing (Original Draft Preparation), C.T., S. L. and M.I.; Writing (Review & Editing), C.T., G.H., M.I., S.L., J. L., N.D., T.L.R, X.X. and I.H.Z.; Project Administration, C.T. and I.H.Z.; Funding Acquisition, C.T. and I.H.Z. All authors have read and agreed to the published version of the manuscript.

Funding: This research was financially supported by the following funding sources: NIH R01 HL153176, and American Heart Association (AHA) CDA (19CDA34520004), and AHA TPA (24TPA1300008; 25TPA1472723).

Institutional Review Board Statement: All animal experimental protocols were approved by the Institutional Animal Use and Care Committee (IACUC) at the University of Nebraska Medical Center (Approval No: # 21-069-10-FC; Approval date: 03 July 2024) and at the University of Kentucky (Approval No: # 2021-3886; Approval date: 03 October 2024) and were carried out in accordance with the NIH guide for the care and use of laboratory animals and with ARRIVE guidelines.

Informed Consent Statement: Not applicable.

Data Availability Statement: The datasets generated and analyzed in this study are publicly available in the NCBI BioProject database under the accession number PRJNA1452487 (https://www.ncbi.nlm.nih.gov/bioproject/PRJNA1452487), accessed on 1 July 2027.

Acknowledgments: We are grateful to Ms. Kaye Talbitzer for her excellent technical assistance in the rodent model of CHF, and Dr. Bryan Hackfort from the Echocardiography Imaging Core at the University of Nebraska Medical Center for echocardiographic assessment and analysis; Dr. Alan Daugherty from the Department of Physiology at the University of Kentucky College of Medicine for providing access to use the departmental Core facility.

Conflicts of Interest: The authors declare that they have no known conflicts of interest. The funders had no role in the design of the study; in the collection, analyses, or interpretation of data; in the writing of the manuscript; or in the decision to publish the results.

References

1. Benjamin, E.J.; Muntner, P.; Alonso, A.; Bittencourt, M.S.; Callaway, C.W.; Carson, A.P.; Chamberlain, A.M.; Chang, A.R.; Cheng, S.; Das, S.R.; et al. Heart Disease and Stroke Statistics-2019 Update: A Report From the American Heart Association. *Circulation* **2019**, *139*, e56-e528, doi:10.1161/cir.0000000000000659.
2. Cannon, J.A.; Moffitt, P.; Perez-Moreno, A.C.; Walters, M.R.; Broomfield, N.M.; McMurray, J.J.V.; Quinn, T.J. Cognitive Impairment and Heart Failure: Systematic Review and Meta-Analysis. *J Card Fail* **2017**, *23*, 464-475, doi:10.1016/j.cardfail.2017.04.007.
3. Harkness, K.; Demers, C.; Heckman, G.A.; McKelvie, R.S. Screening for cognitive deficits using the Montreal cognitive assessment tool in outpatients ≥65 years of age with heart failure. *Am J Cardiol* **2011**, *107*, 1203-1207, doi:10.1016/j.amjcard.2010.12.021.
4. de la Torre, J.C. Alzheimer disease as a vascular disorder: nosological evidence. *Stroke* **2002**, *33*, 1152-1162, doi:10.1161/01.str.0000014421.15948.67.
5. Mokhber, N.; Shariatzadeh, A.; Avan, A.; Saber, H.; Babaei, G.S.; Chaimowitz, G.; Azarpazhooh, M.R. Cerebral blood flow changes during aging process and in cognitive disorders: A review. *Neuroradiol J* **2021**, *34*, 300-307, doi:10.1177/19714009211002778.
6. Alosco, M.L.; Hayes, S.M. Structural brain alterations in heart failure: a review of the literature and implications for risk of Alzheimer's disease. *Heart Fail Rev* **2015**, *20*, 561-571, doi:10.1007/s10741-015-9488-5.

 doi:10.20944/preprints202605.0455.v1

7. Montagne, A.; Barnes, S.R.; Sweeney, M.D.; Halliday, M.R.; Sagare, A.P.; Zhao, Z.; Toga, A.W.; Jacobs, R.E.; Liu, C.Y.; Amezcua, L.; et al. Blood-brain barrier breakdown in the aging human hippocampus. *Neuron* **2015**, *85*, 296-302, doi:10.1016/j.neuron.2014.12.032.
8. Jefferson, A.L.; Liu, D.; Gupta, D.K.; Pechman, K.R.; Watchmaker, J.M.; Gordon, E.A.; Rane, S.; Bell, S.P.; Mendes, L.A.; Davis, L.T.; et al. Lower cardiac index levels relate to lower cerebral blood flow in older adults. *Neurology* **2017**, *89*, 2327-2334, doi:10.1212/wnl.0000000000004707.
9. Havakuk, O.; King, K.S.; Grazette, L.; Yoon, A.J.; Fong, M.; Bregman, N.; Elkayam, U.; Kloner, R.A. Heart Failure-Induced Brain Injury. *J Am Coll Cardiol* **2017**, *69*, 1609-1616, doi:10.1016/j.jacc.2017.01.022.
10. Ovsenik, A.; Podbregar, M.; Fabjan, A. Cerebral blood flow impairment and cognitive decline in heart failure. *Brain Behav* **2021**, *11*, e02176, doi:10.1002/brb3.2176.
11. Almeida, O.P.; Garrido, G.J.; Beer, C.; Lautenschlager, N.T.; Arnolda, L.; Flicker, L. Cognitive and brain changes associated with ischaemic heart disease and heart failure. *Eur Heart J* **2012**, *33*, 1769-1776, doi:10.1093/eurheartj/ehr467.
12. Meng, F.; Zhou, L.; Zhang, B.; Wang, Y.; Bai, Y.; Han, Y.; Wang, L.; Xu, J. Extracellular vesicles as multiorgan crosstalk mediators in cardiovascular diseases: emerging biomarkers and therapeutic targets. *European Journal of Pharmacology* **2025**, *1004*, 177976, doi:https://doi.org/10.1016/j.ejphar.2025.177976.
13. Berumen Sánchez, G.; Bunn, K.E.; Pua, H.H.; Rafat, M. Extracellular vesicles: mediators of intercellular communication in tissue injury and disease. *Cell Commun Signal* **2021**, *19*, 104, doi:10.1186/s12964-021-00787-y.
14. Lago-Baameiro, N.; Camino, T.; Vazquez-Durán, A.; Sueiro, A.; Couto, I.; Santos, F.; Baltar, J.; Falcón-Pérez, J.M.; Pardo, M. Intra and inter-organ communication through extracellular vesicles in obesity: functional role of obesesomes and steatosomes. *J Transl Med* **2025**, *23*, 207, doi:10.1186/s12967-024-06024-7.
15. Kalluri, R.; LeBleu, V.S. The biology, function, and biomedical applications of exosomes. *Science* **2020**, *367*, eaau6977, doi:doi:10.1126/science.aau6977.
16. Kumar, M.A.; Baba, S.K.; Sadida, H.Q.; Marzooqi, S.A.; Jerobin, J.; Altemani, F.H.; Algehainy, N.; Alanazi, M.A.; Abou-Samra, A.-B.; Kumar, R.; et al. Extracellular vesicles as tools and targets in therapy for diseases. *Signal Transduction and Targeted Therapy* **2024**, *9*, 27, doi:10.1038/s41392-024-01735-1.
17. Ruan, J.; Miao, X.; Schlüter, D.; Lin, L.; Wang, X. Extracellular vesicles in neuroinflammation: Pathogenesis, diagnosis, and therapy. *Molecular Therapy* **2021**, *29*, 1946-1957, doi:10.1016/j.ymthe.2021.04.020.
18. Sun, L.L.; Duan, M.J.; Ma, J.C.; Xu, L.; Mao, M.; Biddyut, D.; Wang, Q.; Yang, C.; Zhang, S.; Xu, Y.; et al. Myocardial infarction-induced hippocampal microtubule damage by cardiac originating microRNA-1 in mice. *J Mol Cell Cardiol* **2018**, *120*, 12-27, doi:10.1016/j.yjmcc.2018.05.009.
19. Tian, C.; Gao, L.; Rudebush, T.L.; Yu, L.; Zucker, I.H. Extracellular Vesicles Regulate Sympatho-Excitation by Nrf2 in Heart Failure. *Circ Res* **2022**, *131*, 687-700, doi:10.1161/circresaha.122.320916.
20. Li, Q.; Hamdalla, R.H.; Dhyani, N.; Sun, L.; Gao, L.; Rudebush, T.L.; Zucker, I.H.; Tian, C. Cardiac Injury Regulates Neuroinflammation Through Extracellular Vesicle-Mediated Heart-Brain Crosstalk. *JACC Basic Transl Sci* **2025**, *10*, 101307, doi:10.1016/j.jacbts.2025.05.002.
21. Liao, K.; Yu, J.; Mohammadigoldar, Z.; Li, J.; Liu, W.; Li, L.; Marbán, E. Heart-Brain Crosstalk in Myocardial Infarction: Role of Heart Extracellular Vesicles in Neuroinflammation. *Circ Res* **2025**, *136*, 1513-1515, doi:10.1161/circresaha.125.326237.
22. Tian, C.; Gao, L.; Zimmerman, M.C.; Zucker, I.H. Myocardial infarction-induced microRNA-enriched exosomes contribute to cardiac Nrf2 dysregulation in chronic heart failure. *Am J Physiol Heart Circ Physiol* **2018**, *314*, H928-h939, doi:10.1152/ajpheart.00602.2017.
23. Yelamanchili, S.V.; Lamberty, B.G.; Rennard, D.A.; Morsey, B.M.; Hochfelder, C.G.; Meays, B.M.; Levy, E.; Fox, H.S. MiR-21 in Extracellular Vesicles Leads to Neurotoxicity via TLR7 Signaling in SIV Neurological Disease. *PLoS Pathog* **2015**, *11*, e1005032, doi:10.1371/journal.ppat.1005032.
24. Perez-Gonzalez, R.; Gauthier, S.A.; Kumar, A.; Levy, E. The exosome secretory pathway transports amyloid precursor protein carboxyl-terminal fragments from the cell into the brain extracellular space. *J Biol Chem* **2012**, *287*, 43108-43115, doi:10.1074/jbc.M112.404467.

 doi:10.20944/preprints202605.0455.v1

25. Ge, X.; Meng, Q.; Wei, L.; Liu, J.; Li, M.; Liang, X.; Lin, F.; Zhang, Y.; Li, Y.; Liu, Z.; et al. Myocardial ischemia-reperfusion induced cardiac extracellular vesicles harbour proinflammatory features and aggravate heart injury. *J Extracell Vesicles* **2021**, *10*, e12072, doi:10.1002/jev2.12072.
26. Loyer, X.; Zlatanova, I.; Devue, C.; Yin, M.; Howangyin, K.Y.; Klaihmon, P.; Guerin, C.L.; Kheloufi, M.; Vilar, J.; Zannis, K.; et al. Intra-Cardiac Release of Extracellular Vesicles Shapes Inflammation Following Myocardial Infarction. *Circ Res* **2018**, *123*, 100-106, doi:10.1161/circresaha.117.311326.
27. Kozomara, A.; Birgaoanu, M.; Griffiths-Jones, S. miRBase: from microRNA sequences to function. *Nucleic Acids Res* **2019**, *47*, D155-d162, doi:10.1093/nar/gky1141.
28. Love, M.I.; Huber, W.; Anders, S. Moderated estimation of fold change and dispersion for RNA-seq data with DESeq2. *Genome Biol* **2014**, *15*, 550, doi:10.1186/s13059-014-0550-8.
29. Ru, Y.; Kechris, K.J.; Tabakoff, B.; Hoffman, P.; Radcliffe, R.A.; Bowler, R.; Mahaffey, S.; Rossi, S.; Calin, G.A.; Bemis, L.; et al. The multiMiR R package and database: integration of microRNA-target interactions along with their disease and drug associations. *Nucleic Acids Res* **2014**, *42*, e133, doi:10.1093/nar/gku631.
30. Chou, C.H.; Shrestha, S.; Yang, C.D.; Chang, N.W.; Lin, Y.L.; Liao, K.W.; Huang, W.C.; Sun, T.H.; Tu, S.J.; Lee, W.H.; et al. miRTarBase update 2018: a resource for experimentally validated microRNA-target interactions. *Nucleic Acids Res* **2018**, *46*, D296-d302, doi:10.1093/nar/gkx1067.
31. Agarwal, V.; Bell, G.W.; Nam, J.W.; Bartel, D.P. Predicting effective microRNA target sites in mammalian mRNAs. *Elife* **2015**, *4*, doi:10.7554/eLife.05005.
32. Chen, Y.; Wang, X. miRDB: an online database for prediction of functional microRNA targets. *Nucleic Acids Res* **2020**, *48*, D127-d131, doi:10.1093/nar/gkz757.
33. Yu, G.; Wang, L.G.; Han, Y.; He, Q.Y. clusterProfiler: an R package for comparing biological themes among gene clusters. *Omics* **2012**, *16*, 284-287, doi:10.1089/omi.2011.0118.
34. Dodson, J.A.; Truong, T.T.; Towle, V.R.; Kerins, G.; Chaudhry, S.I. Cognitive impairment in older adults with heart failure: prevalence, documentation, and impact on outcomes. *Am J Med* **2013**, *126*, 120-126, doi:10.1016/j.amjmed.2012.05.029.
35. Vellone, E.; Chialà, O.; Boyne, J.; Klompstra, L.; Evangelista, L.S.; Back, M.; Ben Gal, T.; Mårtensson, J.; Strömberg, A.; Jaarsma, T. Cognitive impairment in patients with heart failure: an international study. *ESC Heart Fail* **2020**, *7*, 46-53, doi:10.1002/ehf2.12542.
36. Goh, F.Q.; Kong, W.K.F.; Wong, R.C.C.; Chong, Y.F.; Chew, N.W.S.; Yeo, T.C.; Sharma, V.K.; Poh, K.K.; Sia, C.H. Cognitive Impairment in Heart Failure-A Review. *Biology (Basel)* **2022**, *11*, doi:10.3390/biology11020179.
37. Grzybowska-Ganszczyk, D.; Nowak, Z.; Opara, J.A.; Nowak-Lis, A. Hypoxia and Cognitive Functions in Patients Suffering from Cardiac Diseases: A Narrative Review. *J Clin Med* **2025**, *14*, doi:10.3390/jcm14196750.
38. Liu, W.; Zhang, X.; Wu, Z.; Huang, K.; Yang, C.; Yang, L. Brain-heart communication in health and diseases. *Brain Res Bull* **2022**, *183*, 27-37, doi:10.1016/j.brainresbull.2022.02.012.
39. Sabayan, B.; van Buchem, M.A.; de Craen, A.J.; Sigurdsson, S.; Zhang, Q.; Harris, T.B.; Gudnason, V.; Arai, A.E.; Launer, L.J. N-terminal pro-brain natriuretic peptide and abnormal brain aging: The AGES-Reykjavik Study. *Neurology* **2015**, *85*, 813-820, doi:10.1212/wnl.0000000000001885.
40. de Bold, A.J.; Borenstein, H.B.; Veress, A.T.; Sonnenberg, H. A rapid and potent natriuretic response to intravenous injection of atrial myocardial extract in rats. *Life Sci* **1981**, *28*, 89-94, doi:10.1016/0024-3205(81)90370-2.
41. Mascolo, A.; Sessa, M.; Scavone, C.; De Angelis, A.; Vitale, C.; Berrino, L.; Rossi, F.; Rosano, G.; Capuano, A. New and old roles of the peripheral and brain renin-angiotensin-aldosterone system (RAAS): Focus on cardiovascular and neurological diseases. *Int J Cardiol* **2017**, *227*, 734-742, doi:10.1016/j.ijcard.2016.10.069.
42. Deng, Z.; Jiang, J.; Wang, J.; Pan, D.; Zhu, Y.; Li, H.; Zhang, X.; Liu, X.; Xu, Y.; Li, Y.; et al. Angiotensin Receptor Blockers Are Associated With a Lower Risk of Progression From Mild Cognitive Impairment to Dementia. *Hypertension* **2022**, *79*, 2159-2169, doi:10.1161/hypertensionaha.122.19378.
43. Althammer, F.; Roy, R.K.; Kirchner, M.K.; Campos-Lira, E.; Whitley, K.E.; Davis, S.; Montanez, J.; Ferreira-Neto, H.C.; Danh, J.; Feresin, R.; et al. Angiotensin II-Mediated Neuroinflammation in the Hippocampus Contributes to Neuronal Deficits and Cognitive Impairment in Heart Failure Rats. *Hypertension* **2023**, *80*, 1258-1273, doi:10.1161/hypertensionaha.123.21070.

 doi:10.20944/preprints202605.0455.v1

44. Redwine, L.S.; Hong, S.; Kohn, J.; Martinez, C.; Hurwitz, B.E.; Pung, M.A.; Wilson, K.; Pruitt, C.; Greenberg, B.H.; Mills, P.J. Systemic Inflammation and Cognitive Decrements in Patients With Stage B Heart Failure. *Psychosom Med* **2022**, *84*, 133-140, doi:10.1097/psy.0000000000001033.
45. AlRawili, N.; Al-Kuraishy, H.M.; Al-Gareeb, A.I.; Abdel-Fattah, M.M.; Al-Harchan, N.A.; Alruwaili, M.; Papadakis, M.; Alexiou, A.; Batiha, G.E. Trajectory of Cardiogenic Dementia: A New Perspective. *J Cell Mol Med* **2025**, *29*, e70345, doi:10.1111/jcmm.70345.
46. Liu, J.; Xiao, G.; Liang, Y.; He, S.; Lyu, M.; Zhu, Y. Heart-brain interaction in cardiogenic dementia: pathophysiology and therapeutic potential. *Front Cardiovasc Med* **2024**, *11*, 1304864, doi:10.3389/fcvm.2024.1304864.
47. Kim, T.; Mehta, S.L.; Morris-Blanco, K.C.; Chokkalla, A.K.; Chelluboina, B.; Lopez, M.; Sullivan, R.; Kim, H.T.; Cook, T.D.; Kim, J.Y.; et al. The microRNA miR-7a-5p ameliorates ischemic brain damage by repressing α-synuclein. *Sci Signal* **2018**, *11*, doi:10.1126/scisignal.aat4285.
48. Zhang, J.; Zhao, M.; Yan, R.; Liu, J.; Maddila, S.; Junn, E.; Mouradian, M.M. MicroRNA-7 Protects Against Neurodegeneration Induced by α-Synuclein Preformed Fibrils in the Mouse Brain. *Neurotherapeutics* **2021**, *18*, 2529-2540, doi:https://doi.org/10.1007/s13311-021-01130-6.
49. Ramesh, M.; Govindaraju, T. MiR-7a-Klf4 axis as a regulator and therapeutic target of neuroinflammation and ferroptosis in Alzheimer's disease. *NAR Mol Med* **2025**, *2*, ugaf022, doi:10.1093/narmme/ugaf022.
50. Shao, X.; Chen, C.; Miao, C.; Yu, X.; Li, X.; Geng, J.; Fan, D.; Lin, X.; Chen, Z.; Shi, Y. Expression analysis of microRNAs and their target genes during experimental diabetic renal lesions in rats administered with ginsenoside Rb1 and trigonelline. *Pharmazie* **2019**, *74*, 492-498, doi:10.1691/ph.2019.8903.
51. Bostjancic, E.; Zidar, N.; Stajer, D.; Glavac, D. MicroRNAs miR-1, miR-133a, miR-133b and miR-208 are dysregulated in human myocardial infarction. *Cardiology* **2010**, *115*, 163-169, doi:10.1159/000268088.
52. Carè, A.; Catalucci, D.; Felicetti, F.; Bonci, D.; Addario, A.; Gallo, P.; Bang, M.L.; Segnalini, P.; Gu, Y.; Dalton, N.D.; et al. MicroRNA-133 controls cardiac hypertrophy. *Nat Med* **2007**, *13*, 613-618, doi:10.1038/nm1582.
53. Crocco, P.; Montesanto, A.; La Grotta, R.; Paparazzo, E.; Soraci, L.; Dato, S.; Passarino, G.; Rose, G. The Potential Contribution of MyomiRs miR-133a-3p, -133b, and -206 Dysregulation in Cardiovascular Disease Risk. *Int J Mol Sci* **2024**, *25*, doi:10.3390/ijms252312772.
54. Zhu, Y.; Xu, Q.; Sha, W.P.; Zhao, K.P.; Wang, L.M. MiR-219-5p promotes spinal cord injury recovery by inhibiting NEUROD2-regulated inflammation and oxidative stress. *Eur Rev Med Pharmacol Sci* **2019**, *23*, 37-43, doi:10.26355/eurrev_201901_16745.
55. Liu, N.; Zhou, Q.; Wang, H.; Li, Q.; Chen, Z.; Lin, Y.; Yi, L.; Jiang, S.; Chen, C.; Deng, Y. MiRNA-338-3p Inhibits Neuroinflammation in the Corpus Callosum of LCV-LPS Rats Via STAT1 Signal Pathway. *Cell Mol Neurobiol* **2023**, *43*, 3669-3692, doi:10.1007/s10571-023-01378-w.
56. Zhu, M.; Ye, L.; Zhu, G.; Zeng, Y.; Yang, C.; Cai, H.; Mo, Y.; Song, X.; Gao, X.; Peng, W.; et al. ROS-Responsive miR-150-5p Downregulation Contributes to Cigarette Smoke-Induced COPD via Targeting IRE1α. *Oxid Med Cell Longev* **2022**, *2022*, 5695005, doi:10.1155/2022/5695005.
57. Duroux-Richard, I.; Roubert, C.; Ammari, M.; Présumey, J.; Grün, J.R.; Häupl, T.; Grützkau, A.; Lecellier, C.H.; Boitez, V.; Codogno, P.; et al. miR-125b controls monocyte adaptation to inflammation through mitochondrial metabolism and dynamics. *Blood* **2016**, *128*, 3125-3136, doi:10.1182/blood-2016-02-697003.
58. Zhang, Q.; Yu, K.; Cao, Y.; Luo, Y.; Liu, Y.; Zhao, C. miR-125b promotes the NF-κB-mediated inflammatory response in NAFLD via directly targeting TNFAIP3. *Life Sciences* **2021**, *270*, 119071, doi:https://doi.org/10.1016/j.lfs.2021.119071.
59. Bamahel, A.S.; Sun, X.; Wu, W.; Mu, C.; Liu, J.; Bi, S.; Xu, H. Regulatory Roles and Therapeutic Potential of miR-122-5p in Hypoxic-Ischemic Brain Injury: Comprehensive Review. *Cell Biochem Biophys* **2025**, *83*, 2651-2668, doi:10.1007/s12013-025-01686-6.
60. Song, W.; Zhang, T.; Yang, N.; Zhang, T.; Wen, R.; Liu, C. Inhibition of micro RNA miR-122-5p prevents lipopolysaccharide-induced myocardial injury by inhibiting oxidative stress, inflammation and apoptosis via targeting GIT1. *Bioengineered* **2021**, *12*, 1902-1915, doi:10.1080/21655979.2021.1926201.
61. Hu, Y.; Du, G.; Li, G.; Peng, X.; Zhang, Z.; Zhai, Y. The miR-122 inhibition alleviates lipid accumulation and inflammation in NAFLD cell model. *Arch Physiol Biochem* **2021**, *127*, 385-389, doi:10.1080/13813455.2019.1640744.

 doi:10.20944/preprints202605.0455.v1

62. Hu, Y.; Peng, X.; Du, G.; Zhang, Z.; Zhai, Y.; Xiong, X.; Luo, X. MicroRNA-122-5p Inhibition Improves Inflammation and Oxidative Stress Damage in Dietary-Induced Non-alcoholic Fatty Liver Disease Through Targeting FOXO3. *Frontiers in Physiology* **2022**, *13*, doi:10.3389/fphys.2022.803445.
63. Hu, S.; Hu, Y.; Yan, W. Extracellular vesicle-mediated interorgan communication in metabolic diseases. *Trends in endocrinology and metabolism: TEM* **2023**.
64. Mo, W.; Peng, Y.; Zheng, Y.; Zhao, S.; Deng, L.; Fan, X. Extracellular vesicle-mediated bidirectional communication between the liver and other organs: mechanistic exploration and prospects for clinical applications. *Journal of Nanobiotechnology* **2025**, *23*, 190, doi:10.1186/s12951-025-03259-4.